

84-36.3

ADVANCES IN THE CHARACTERIZATION AND
CONTROL OF EMISSIONS FROM PRESCRIBED FIRES

DAROLD E. WARD

COLIN C. HARDY

UNITED STATES DEPARTMENT OF AGRICULTURE
SEATTLE, WASHINGTON



For Presentation at the 77th Annual Meeting of the
Air Pollution Control Association
San Francisco, California June 24-29, 1984

INTRODUCTION

Progress is being made in characterizing emissions from the prescribed broadcast burning of logging slash in the Pacific Northwest. To accomplish the characterization work, it was necessary to establish specific test units on which the mass of residues to be burned was reduced by yarding to various minimum-piece-size specifications. Our primary objective was to measure the reduction in emissions produced from burning incrementally smaller amounts of residues on units where the timber had been harvested. Improvements in air quality can be achieved through increased utilization of residues, but it is only because of the emissions characterization work of recent years that this hypothesis can be validated and calibrated.

Fires used to burn forest biomass wastes in the open environment produce an abundance of fine particles and incompletely oxidized combustion products.¹ In this paper, along with emission factors and source strength data for the primary combustion products, data are presented for benzo[a]pyrene (b[a]p) and a number of trace elements. We discuss new information on the mass of particulate matter (PM-2.5) produced below a mean mass diameter of 2.5 μm . Even though prescribed fires are planned events with weather factors, fuel conditions, and firing patterns specified, acquiring empirical data for the full-scale prescribed burn is difficult. A thorough characterization of emissions is important to forest and air resource managers alike because the benefits of prescribed fire accrue to forest management and have been determined to be economically favorable.² At the same time, however, adverse effects on air quality must be minimized by selecting the appropriate prescription for the prescribed burn to minimize the production of pollutants and take advantage of optimal dispersion conditions.³

Air resource managers need reliable data to assess the relative impact of sources such as prescribed fires on air quality at receptor sites. In western Washington and Oregon, receptor modeling is being practiced by regional air pollution control authorities, and prescribed fire seems to be a major contributor to air-quality degradation during the prescribed-burning season--May to November.⁴ In this paper, we discuss emissions of trace constituents that are important to the receptor modeling process.

Fire management staff need algorithms to predict the quantity of emission reduction that can be achieved by using various burning techniques. Information on production of emissions by combustion phase is needed for the primary combustion products including PM, CO, and b[a]p. There is a tremendous difference in the rate of production between flaming and smoldering processes; hence, it is important to quantify, by combustion phase, the following variables: emissions production, fuel consumption, and heat release rate over time. New information on emissions production as a function of time, fuel, and weather variables is presented in this paper, which supplements the work of Sandberg⁵ and Ward.⁶ We are now able to describe functions which are useful in assessing the emissions production from broadcast burning of logging slash in western Washington and Oregon.

New data and trends describing relationships and models are discussed in this paper; however, the results must be considered preliminary because five to six additional test fires are scheduled for summer 1984. A final report will be presented after the 1984 test program. Publications are planned that will provide a more comprehensive treatment of emission factors, production of trace elements, production of trace gases, production of b[a]p and complete polycyclic aromatic hydrocarbon (PAH) profiles, and the development of models for predicting emissions production for prescribed fires used to broadcast burn logging slash.

BACKGROUND

At this conference last year, McMahon¹ summarized what is known about the chemical and physical characteristics of smoke from forest fires and made the point that the variability of emissions production is largely influenced by the fuels consumed. Emission factors for various components of smoke from prescribed fires can be influenced by planning the fire to take advantage of specific weather and firing techniques. Through such planning, emissions can be reduced by at least 35%.⁵

Detailed characterization of emissions from prescribed fires began in the early 1970's with published accounts by Fritschen and others⁷ in the Pacific Northwest, by Ward and Lamb⁸ in the Southeast, and by Vines and others⁹ in Australia. Included in the observations by Fritschen and others⁷ are measurements of emission factors derived from small-scale laboratory tests for PM, CO, CO₂, and hydrocarbons. Their observations show emission factors lower than those measured by Sandberg¹⁰ and Ward and others.¹¹ Sandberg and others¹² report on trace hydrocarbon emissions from the combustion of fuels treated with fire retardants and burned under a combustion hood.

Problems exist in comparing results from studies using combustion hoods with those from full-scale prescribed fires. Comparisons between emission factors derived from laboratory tests and field fires show agreement only when fuel and fire behavior scaling are similar. Layering of forest fuels, moisture content gradients, and the arrangement of fuel particles affect fire behavior and emissions production.¹³ The problem associated with applying combustion laboratory results to the full-scale phenomena has been one of the major motivating factors in developing field techniques^{1,14} for measuring emissions.¹⁵ These procedures use techniques that measure the flux of emissions and the carbon-mass balance with a specialized sampling system.

The use of the carbon-mass balance technique for measuring emissions was pioneered in burning grass and stubble¹⁶ and perfected^{9,13} for field use with prescribed forest fires. Nelson¹⁷ evaluated the carbon-mass balance method using prepared replicated fuel beds burned in a combustion laboratory. The measured fuel consumption for the total fire was within 15% of the carbon-mass balance values. Nelson did not report the accuracy by combustion phase. The relatively narrow range of carbon content of forest fuels (45% to 55%, by weight) allows accurate measurement of emissions. Three methods for measuring emission factors in the field were compared, and emission factors determined using the carbon-mass balance procedure agreed well with emission factors determined by dividing the measured fuel consumption into the measured emissions flux.¹⁸ Emission factors measured from towers over prescribed fires were compared with emission factors from sampling the fuel consumption and PM flux. Observations of PM flux were made by flying a sampling system through the smoke plume. Agreement was very good for these tests. It is basically because of these successes that Ward and others¹⁸ incorporated equipment for measuring the vertical velocity into their sampling system. We expanded the methods to accommodate for real-time measurements of gases and PM.

METHODS:

The data presented in this paper were collected from 6 test areas (each about 0.2 hectare) where emission factors and the flux of emissions were measured over the duration of the test fires. The tests were all on logged units in western Oregon and were selected to represent a range of fuel bed conditions (fuel loading, fuel moisture, and extent of yarding of unmerchantable material) and weather conditions that would provide a wide range of combustion environments (fire intensity, fire duration, and smoldering potential). Four of these logged units were independently located with two of the units having two treatments (to test for the effect of fuel moisture on emissions production). Data describing the test areas are in Table I.

A combination of in-situ continuous and removable sampling techniques were employed to: (1) account for the mass flux of all carbon-bearing gases and particles; (2) measure the rates of energy release and convective flow; (3) remove samples for chemical analysis to quantify changes in the chemical composition of the smoke traceable to changes in the combustion environment; and (4) to calibrate the sensors for continuous measurement of the emissions concentration.

Particulate matter and gaseous emissions were sampled by suspending packages containing multiple sensors over areas to be burned. Two types of packages were used: (1) those containing samplers for real-time measurements of parameters, and (2) those that were periodically removed from the sample environment to replace filters and gas sample bags. (Real-time is defined as sampling with a sample intensity of at least one set of observations each 30 seconds.) The two sets of packages were aligned over the area to be sampled so that respectively numbered packages from each system were nominally in the same sample space (Figure 1). In the past, sampling procedures have used only a grab-sample system.¹¹ During 1983, a real-time system was placed in operation that improved the resolution of emissions-production characterization over time--especially during the period of transition from flaming to smoldering when the rate of fuel consumption is still near a maximum. Both systems were elevated to 15 m (50 ft) above the ground for the flaming phase and were then lowered to about 9 m (30 ft) for sampling of smoldering phase emissions.

Carbon-Mass Balance

A fundamental assumption is that the carbon in forest fuel is released in a one-to-one proportion to the carbon of the emissions produced, and the emissions are well mixed in the atmosphere. By measuring the concentration of carbonaceous gases and PM, the carbon contained in a unit volume (cubic meter) of air can be derived and converted to the equivalent mass of fuel consumed in producing the combustion gases. We know, from samples taken of the forest fuel before and after burning, that the forest fuel and the ash residues have very nearly the same carbon content (40% to 55% carbon by weight, respectively).

A low-flow pulse pump, which fills a 5-liter, aluminized-mylar, gas-sampling bag over a predetermined time interval was located in each of the packages used to take grab samples. We used a Baseline Industries Model 1030A gas chromatograph (Mention of trade names throughout this Paper does not constitute endorsement by the U. S. Department of Agriculture), a Horiba Model PIR-2000 nondispersive infrared gas analyzer, and either an Ecolyzer Model 2100 or an Interscan 1140 to analyze the gases for NMHC and CH₄, CO₂, and CO, respectively. The concentration of carbonaceous gases is differentiated from gases in the background air by collecting a representative number of background air samples.

Two personal pumps in each package were used for collecting PM-2.5 and PM samples on filters simultaneously with the samples for gas analysis. One pump in each package was fitted with a tared 47-mm Gelman Type A glass fiber filter mat and operated at a flow rate of 3.5 l per minute (l/m). The other pump, operated at 2.0 l/m, used a 2.5 μ m mean mass diameter cut-point cyclone with tared 37-mm filter mats. (Throughout this Paper, the results for the samples collected without the cyclone pre-sampler are referred to as PM samples; whereas, the samples collected with the cyclone pre-sampler in place are referred to as PM-2.5 samples.) For a given grab sample, three stretched-TEFLON filters were used to collect samples for X-ray fluorescence analysis of trace elements and two glass fiber filters were used for analysis of the organic and elemental carbon content of the PM-2.5.

Real-time measurement of CO and CO₂ concentrations was accomplished, in situ, by pumping gaseous emissions at each continuous sampling package to a train of gas analyzers along one edge of the prescribed fire. The analog signals from the CO and CO₂ analyzers were recorded on a data logger for later conversion to appropriate engineering units. In addition, a personal-sized airborne particulate monitor was included in each of the five,

real-time, continuous instrument packages for the purpose of measuring the PM concentration. These ultra-compact, microprocessor-based aerosol monitors (MINIRAMS) measure light scattering of particles and are most sensitive to particles ranging in size from 0.1 to 10 μm . Each MINIRAM provided a continuous, real-time analog signal proportional to the aerosol concentration. The analog output signal from each monitor was recorded by the data logger. The recorded MINIRAM analog response was calibrated against gravimetric filter samples of the PM-2.5 which were collected adjacent to, and concurrently with, the real-time monitoring. As was predicted, PM-2.5 concentrations determined from gravimetric weighing of the exposed 37-mm filters provided the highest correlation coefficient with the MINIRAM response (R-squared of 0.73).

Carbon Mass Flux

Fuel consumption and emissions source strength were calculated by measuring the flux of carbon through an imaginary horizontal plane. The real-time sampling system provided a technique for quantifying carbon mass flux as a function of time. The carbon mass was computed by summing the carbon fraction of the measured CO, CO₂, and PM concentrations for a given instrument package at a given time. The recorded analog responses from the CO analyzer, CO₂ analyzer, and each of the five MINIRAMs provided a real-time representation of the respective gas and PM concentrations.

The vertical component of the convection column velocity was measured continuously by a mass-flow-velocity probe installed at each real-time instrument package. Each velocity probe was fitted with a cylindrical shroud designed to protect the probe from the horizontal wind component. The shroud design was tested in a low-speed wind tunnel to determine the response of the velocity probe as the shroud was rotated 90° to the nominal direction of the wind. An approximate cosine response was verified.¹¹ The sensing element of the probe consisted of a velocity sensor and a temperature sensor. The velocity sensor was heated and responded to standard velocity (25 °C and 760 mmHg); the temperature sensor compensated for ambient temperature. The design provided accurate mass-flow measurements of the vertical plume under a wide range of ambient temperatures (-55 to +325 °C). The flux of carbon per unit area for a given period was computed by multiplying the measured vertical plume by the carbon concentration. Specific equations for computing fuel consumption by the carbon-mass flux method are discussed below.

RESULTS AND DISCUSSION

Emission production rates are a function of the appropriate emission factor multiplied by the rate of fuel consumption. The rate of fuel consumption, total mass of fuels consumed, and the emissions produced are functions of the fuel properties and weather. Fire duration is also a function of the available fuel which is determined largely by the moisture content of the fuel complex. Mathematical equations are fit to the measured rate of fuel consumption. It is believed that expressions can be developed for predicting the rate of fuel consumption as a function of time based on readily predictable parameters. Parameters affecting fuel consumption and duration of the smoldering combustion phase are discussed only in a general sense. Refer to work by Sandberg and Ottmar^{19,20} for a more comprehensive treatment of the factors affecting fuel consumption and for algorithms for predicting this phenomenon.

Emission Factors from Grab Samples

Emission factors reported in Tables II and III are based on the mass of emission produced per mass of fuel consumed. These data are for six separate tests. Two of these tests were to sample the emissions from a second treatment that was designed to test the effect of a change in fuel moisture content on emissions production and fuel consumption. The MARIA and DLAKE test areas are described in the Tables and in the text by a number 1 or 2 that indicate the areas were revisited and test fires burned under a second set of moisture conditions. For all the tests, at least one set of grab samples was collected in the flaming combustion phase and one in the smoldering combustion phase. If the smoldering condition persisted, then additional samples were taken during the latter stages of the smoldering period.

The carbon-mass balance method was used exclusively to determine the mass of fuel consumed in producing the concentration of carbon-containing gases. Although fuel takes on the units of mass per unit volume, the number actually represented the fuel consumed to produce the emissions contained in a unit volume (one cubic meter) of gas. This was calculated by summing the carbon content of each of the emissions, C_n , in the unit volume according to equation (1) and dividing by the fuel carbon ratio, R , as follows:

$$W_v = (\sum C_n)/R; \quad (1)$$

where,

W_v = fuel consumed, mg m⁻³,

C_n = the carbon fraction of the emissions, mg m⁻³,

n = CO₂, CO, NMHC, CH₄, PM, and

R = the carbon fraction of the fuel elemental analysis,

0.497 g of carbon per g of fuel, is based on the generalized chemical formula (C₆H₉O₄) for forest fuel.²¹

Emission factors (EF_n) were calculated by dividing the mass of emissions produced by the total fuel consumed to produce the emissions and can be expressed in units of g kg⁻¹ as follows:

$$EF_n = E_n/W_v; \quad (2)$$

where,

EF_n = emission factor of the emission n , g kg⁻¹,

E_n = concentration of emissions n , mg m⁻³,

n = CO₂, CO, NMHC, CH₄, PM, and

W_v = fuel consumed, g m⁻³.

Column 3, Table II, shows that the carbon concentration varied over the duration of each test fire. This measurement was highly sensitive to the CO₂ concentration level above background. For example, for the test located at CAT, three sets of grab samples were taken. The carbon concentration declined for each successive sample as follows: 746, 216, and finally 65 mg m⁻³, respectively, for the flaming and two subsequent smoldering periods. The reliability of the emission factors is judged to be better for those values with higher concentrations of carbon. The carbon content in mass per unit volume of CO₂, CO, and CH₄ is simply the concentration (volume per volume) applied through the Ideal gas law to compute mass concentration. The NMHC are listed in terms of methane. The emission factors for gases, b[a]p, and trace elements are presented in subsequent sections.

For the PM-2.5, the carbon content ranged between 39 and 69% and averaged 54 ±3% for flaming and 47 ±3% for smoldering. Techniques described by Johnson and Huntzicker²² were used to determine the relative mass of elemental and organic carbon content of the PM-2.5. An average value of 50% was used in the calculations to compute the contribution of carbon from the PM-2.5 to the total carbon. This is significantly lower than others have used.^{13,11,17,23} Emission factors (EF_n) calculated by the carbon-mass balance

method can be adjusted for differences in percent carbon of the PM by using equation (3) as follows:

$$EF_{na} = EF_{nb} / (1 + EF_{PMB} * R * (\theta - \beta)); \quad (3)$$

where,

- PM = particulate matter,
- β = new carbon content of PM,
- θ = old carbon content of PM,
- a = new data,
- b = old data,
- n = the specific emission, and
- R = carbon fraction of fuel (see equation 1).

Particulate Matter. EF_{PM} values from Table III were averaged for the flaming combustion phase for the PM-2.5 and PM filter samples. The PM-2.5 samples were collected with filter holder cassettes that had a cyclone in line which prevented aggregates of ash from reaching the filters. Average emission factors were calculated for the flaming phase of 11.2 ± 3.9 and 16.8 ± 6.3 g kg⁻¹ for the PM-2.5 and PM, respectively. A paired t-test showed a significant difference between the two sets of emission factor data at the .05 level of confidence. The percent difference in PM mass between the two sets of filter samples is a function of reaction intensity, the rate of energy release per unit area per unit time (often expressed in kw m⁻²), and is shown in Figure 2 ($\Delta PM = 2.0 * I_r - 57.8$ with an R-squared = .81). Basically, this conclusion is in agreement with the concept that more giant particles (or ash) are entrained in the plumes of higher intensity fires.²³ The strictest definition for reaction intensity, I_r , suggests that I_r should only apply to the highest energy release period for a fire. However, the term has grown in acceptance and is commonly used to describe the energy release rate on a unit area basis as a function of time and has proven to be a valuable parameter to integrate those fire variables that control emissions production.^{10,12}

The increase in PM production that occurred with increased green fuel consumption is illustrated in Figure 3. Because the mass of green fuel was not measured for the 1983 tests, an estimate of relative abundance (0 to 1.0) had to be used as the independent variable. A unit with a high percentage composition of green fuel was rated with a 1.00; and a unit with a lower percentage green fuel component received a proportionately lower rating. The data from the 1982 tests are included in Figure 3 and emission factors for PM increase linearly as green fuel consumption increases.

We hypothesized that ash was entrained in the convection column and was sampled with the PM by the open-faced, 47-mm filters which likely explains some of the variance shown in Figure 3. The same general relationship holds for the samples collected with the PM-2.5, 37-mm filters, except that the relative magnitude of the sloped line is lower and the slope is flatter. We have shown that the percent difference between emission factors for PM-2.5 and PM without size segregation is a function of reaction intensity. Obviously, since the same paired samples have been used to develop the best-fit linear curves in Figure 3, then the difference between sloped-lines must be partly explainable because of the reaction intensity effect. However, since the dependent variable in Figure 3 is the absolute value for each emission factor (not the percent difference) the slope of the lines for the size-segregated samples is a function of green fuel abundance. The test fire with the highest reaction intensity produced the lowest $EF_{PM-2.5}$. But, there were also test fires with large amounts of green fuel that burned with high reaction intensities and produced higher EF_{PM} . This result probably does not apply for conditions of uniform fuels burned under different weather conditions to produce a range of fire intensities. Sandberg¹⁰ found emission factors for PM to be inversely proportional to reaction intensity. This relationship may hold as we perform tests for conditions where the fuel bed characteristics are more nearly similar.

Combustion Gases and Combustion Efficiency. Emission factors for the gases (CO, CH₄, and NMHC) were much lower during the flaming phase than during the first smoldering phase. EF_{CO} , EF_{CH_4} , and EF_{NMHC} correlated negatively with IR. Table II shows that EF_{CO} was lowest (56g kg⁻¹) for the test that had the highest fire intensity during the flaming phase. EF_{CO} values varied by less than a factor of two for the flaming phase and were consistently above 200 g kg⁻¹ for the smoldering phase.

Combustion efficiency is defined in terms of the ratio of the carbon converted to the most highly oxidized form--CO₂. It is a calculated parameter that ranges from 0 to 1.0 and, for prescribed fires, normally ranges from 0.6 to 0.95. Fuel parameters, ignition parameters, and factors affecting fire behavior tend to affect combustion efficiency most directly. Combustion efficiency may be proportional to IR. EF_{CO} values are inversely proportional to combustion efficiency. The relationship is expected because CO is normally the second most abundant gas produced. If all of the carbon were converted to CO, the EF_{CO} would be approximately 1167 g kg⁻¹ and would equal the y-intercept. Our regression equation shows a y-intercept lower ($EF_{CO} = 991.6 - 1005.0 * \text{combustion efficiency}$ with an R-squared of .98) than the theoretical value, which indicates the presence of other incompletely

oxidized compounds; i.e., hydrocarbons and PM. We have found several parameters to be well correlated with combustion efficiency including CO (Figure 4) and a key variable discussed in the next section--the potassium-to-iron ratio.

Trace Elements and Ratios. There are certain ratios of elements in the PM that are unique to a given source; these are referred to as "fingerprints." For source apportionment to be effective, the emission "fingerprints" impacting the receptor must be sufficiently unique to assure model resolution. Impacts from chemically similar sources cannot be concurrent, if their individual contributions are to be resolved. Prescribed fire smoke collected on filters consists of a high percentage of volatilizable organic material. There are also trace elements that are volatilized during the prescribed fires. These elements may reach highly oxidized states, such as CO₂, and be lost from the burn site as gases. Or the elements may be attached to carbonaceous particles and be sampled with the PM on filter substrates. X-ray fluorescence techniques make it possible to measure the abundance of the trace elements contained in the PM and to assess the probability of using one or more of the elements as a tracer material.

Jenkins²⁴ and Cooper and associates⁴ have used the ratio of potassium to iron through an analysis of the enrichment of these elements as an indicator of the contribution of smoke from slash burns to air quality. We examined this combination of elements and found that the abundance of potassium increased with increasing reaction intensity, whereas iron production was not readily correlated with the parameters measured. By plotting the K/Fe ratio as a function of combustion efficiency (Figure 5b), we find an R-squared of .71 for the best-fit equation where $\text{LOG}(K/\text{Fe-ratio}) = 6.46(\text{combustion efficiency}) - 4.15$. It would be desirable to find a "fingerprint" for forest fire smoke that shows less variability than the K/Fe ratio.

The relative abundance of K and Fe in the PM as a function of measured levels of reaction intensity is illustrated by Figure 5a. The PM is enriched with K in proportion to the increase in fire intensity ($\text{EF}_K = 1.55 \times \text{IR} - 29.3$ with an R-squared of 0.69), whereas iron is nondescript. Production rates of K and Fe for prescribed fires would therefore be expected to vary (not be proportionally produced) over the duration of a prescribed fire (Table III). The coefficient of variation for K/Fe, K/PM, and Fe/PM ratios are 200%, 125%, and 181%, respectively. This indicates that the variation in K and Fe content of the PM is not uniform. The range of K/Fe ratios shown in Figure 5b covers nearly three orders of magnitude and is correlated with combustion efficiency. We believe that the Fe is transformed to gaseous species or that the K is combined to a greater extent with the PM for conditions where an

abundance of the carbon is converted to CO₂, as occurs for the higher combustion efficiency fires. One source of variation of Fe may be in the amount of crustal component (dust and soil) introduced through harvesting of the timber.

Where emission factors for K increase in response to fire intensity, a curvilinear and a constant trend are hypothesized for S and P emission factors, respectively (Figures 5a and 5c). It is possible that a higher percentage of the S is converted to SO₂ for the higher fire intensity conditions. Ward and others²⁵ found a negative correlation between carbonyl sulfide (COS) production and reaction intensity for test fires studied in a controlled-environment combustion laboratory. Our observations of higher sulfur content of the PM for the mid-range intensity fires may be consistent with the observations of decreased COS production for similar fire intensities. Many thermodynamic properties are responsible for the kinetics of the chemical reactions and the end products that result. Equilibrium constants and temperatures along the trajectories that the combustion products follow from pyrolysis to quenching in the atmosphere are not well known. Probably the heterogeneous mixture of compounds is so complex as to make a thermodynamic and reaction kinetics approach to predicting chemical reactions and end products fruitless.

Benz[a]pyrene (b[a]p). Our results for field sampling indicated an emission factor range for b[a]p of one order of magnitude (or 125 to 694 µg kg⁻¹). McMahon and Tsoukalas²⁶ studied PAH production in a series of test fires in a controlled-environment combustion laboratory. Their tests of simulated heading and backing fires for pine needle litter fuels showed emission factors for b[a]p ranging from 238 to 3454 µg kg⁻¹ of fuel consumed in backing fires and from 38 to 97 µg kg⁻¹ in heading fires. As illustrated in Figure 6, there is an indication that b[a]p production is correlated with the amount of green fuel in the fuel complex. Many sites in western Washington and Oregon are covered by an understory component of shade-tolerant species. The vegetation often is released at the time of harvesting and grows vigorously. If the unit is not burned and planted during the first year following harvesting of the timber, a much larger amount of green fuel will be present to be burned at a later date with the potential for higher emission rates for both b[a]p and PM (Figures 3 and 6).

Our sampling system was designed to collect samples of PM for b[a]p analysis using four different pump and filter combinations. Our results are preliminary because the analyses for some of the filter samples are not back from the laboratory. We collected two sets of filters with polyurethane foam (PUF) backup filters behind the glass-fiber 47-mm filters to capture b[a]p if

breakthrough were to occur. We also measured the temperature at the sample point, which should help in interpreting the conditions that were present if any breakthrough occurred. In addition to the series of 47-mm glass fiber filters that were collected for each combustion phase, a 0.20- x 0.25-m (8- x 10-inch) glass fiber filter mat was exposed at the same sample location as the PUF and package number one. The 0.20- x 0.25-m filter hi-vol pump was operated at 1.27 cubic meters per minute (45 cubic ft per minute) to collect as large a mass of PM as possible for a complete profiling of the particulate PAH compounds. The profiling work is in progress.

Rate of Fuel Consumption and Emissions Production as a Function of Time

Our method for measuring fuel consumption and emissions production concurrently as a function of time from undisturbed fuel beds was unique. There has always been concern for accurately modeling combustion phenomena in the laboratory so that combustion processes can be adequately described. Our system allows for characterization of the emissions under field conditions with a minimum amount of disturbance to the fuel bed. To characterize fuel consumption as a function of time, it is necessary at a minimum, to measure CO₂, CO, and vertical velocity of the smoke plume immediately over the fire. Temperature and PM concentration are also measured in real time for each of the sample packages. Figure 7 illustrates for MARIA1 the measured fuel consumption, temperature, vertical velocity of the smoke plume, combustion efficiency and emission factors for CO, CO₂, and PM. All variables were measured in real time for each of the test fires. The time periods for which grab samples were collected are included on the diagram.

Many factors interacted to produce the data displayed as a function of time in Figure 7. For example, the indicated rate of fuel consumption is expressed in units of g m⁻² s⁻¹. The measured fuel consumption, however, is an average over an area that projects outward from underneath the sampling system. We believe that the emissions sampled originated in an approximately binomial distribution of increments of time from a series of unit areas extending along the slope on a given contour line. Because of the plume buoyancy and the slope interaction (occasionally a 40% slope), however, the emissions had a tendency to concentrate near the upper part of the slope. We think this did not affect the validity of the sample because the sample packages were located in a systematized grid so that the effect of concentration gradients tended to be minimized through the data averaging procedure. As with any hand-lit prescribed fire, however, the lines of fire take time to coalesce. This is different from laboratory experiments in which a unit area fuel bed is

mass ignited or a line of fire is carefully ignited and allowed to advance a specified distance through a fuel array. Many handlit prescribed fires do, however, use a series of lighters who work across the slope in tandem, and it is common for a swath of 30 to 60 m (100 to 200 ft) in width to be ignited during one pass by four or five lighters--a distance comparable to the distance down the slope covered by our sample packages. The delay in time for the lines of fire to coalesce is integrated by the fuel consumption curve in Figure 7. In all cases, however, our test units were ignited as rapidly as possible.

Combustion rates for undisturbed fuel beds had never before been measured. Large weighing systems had been outfitted with fire-resistant platforms and used to monitor weight loss during the combustion of heavy fuels arranged on the platform, but weight loss from litter, duff, logging slash, and green vegetation with natural moisture gradients and variations in arrangement had not been sampled in real time. Measured combustion rate peaks were somewhat lower and broader than those predicted from laboratory experiments. The suppressed peak combustion rates can be explained, in part, by the averaging process both temporally and spatially. The IR measurements shown in Table II are averages for the sample periods (e.g., as shown in Figure 7).

We had expected a greater range of the variance of EF_{PM} over time. The EF_{PM} increased but at a slower rate than anticipated, and it did not seem to make an abrupt change during the transition from flaming to smoldering combustion. This unexpectedly slow change in the magnitude of the emission factors may be, in part, an artifact of the area averaging phenomena resulting from our sampling technique.

Combustion efficiency, on the other hand, was almost perfectly correlated positively with EF_{CO_2} and negatively correlated with EF_{CO} . The difference between a perfect inverse correlation and actual is the effect of the variance caused by the range in hydrocarbon and PM emission factors.

Source Strength. Source strength (emission rate) per unit area, q , is a function of fuel consumption and emission factor and is expressed in terms of a particular measured emission component (CO, CO₂, PM, etc.). We calculated the flux of the carbon-bearing species over short periods and then summed these to develop total emissions of carbon by species from the fire. By summing the contribution of each of these carbonaceous compounds and by knowing the carbon content of the forest fuel, the fuel consumption can be calculated over short time increments and these summed as follows:

$$W = \int_{t_1}^{t_n} \dot{w} dt \approx \sum_{t_1}^{t_n} \dot{w}(t_n - t_{n-1}); \quad (4)$$

where,

W = total fuel consumed, g m⁻²,

\dot{w} = the rate of fuel consumption per unit area, g m⁻² s⁻¹,
or $\dot{w} = Vz \cdot C/R$,

Vz = the rate of plume rise in the vertical component, m s⁻¹,

C = the carbon concentration, g m⁻²,

$R = 0.497$ based on Byram's²¹ generalized
chemical formula for wood, C₆H₉O₄, and

t = time intervals from n-1 to n, hr.

Cumulative percent consumption over various time intervals can be interpreted from Figure 7 by examining the length of time since ignition and percent consumption associated with that time interval. Reaction intensity, IR , is calculated by multiplying the rate of fuel consumption by the heat value for the fuel (13.95 kJ g⁻¹). Average values of IR were calculated for the periods of time when grab samples were collected and IR used to regress against dependent variables as already discussed for trace elements. Although we have not corrected our calculations of IR based on combustion efficiency, the effect of incomplete combustion can be factored into the IR calculations.

Emission rates or source strength per unit area is a function of fuel consumption and emission factors. The appropriate emission factor to be applied is a function of combustion phase and fire intensity. Hence, source strength per unit area, q , is equal to the rate of fuel consumption, \dot{w} , times the EF for the combustion phase and the component emission (PM, CO, etc.). Equation (5) describes the calculation method for source strength:

$$q = \dot{w}(EF_y) \quad (5)$$

where,

q = source strength per unit area, g m⁻² s⁻¹,

n = CO, PM, etc., and

y = flaming or smoldering.

Examples of q for CO and PM are plotted in Figure 7. In order to predict total emissions and total heat release from a large prescribed fire, it is important to be able to sum up the individual square meters for a prescribed fire unit as it is ignited and describe both the total heat release rate and the total source strength, Q , for the entire unit as a function of time. The rate of ignition and

burnout of the fuel particles are very important variables to characterize. Q is noted to be proportional to the total area on fire for any given time and is the sum of the increment source strength values, q , involved in flaming and smoldering.⁵

Curve Fitting of Functions to Measured Fuel Consumption. Methods are needed for predicting the rate of fuel consumption as a function of time, fuel, and weather variables to reliably predict source strength. In this section, we will fit a set of mathematical equations to the observed rate of fuel consumption over time for four test fires. The variation in the rate of fuel consumption over time is the most important variable to characterize for determining source strength. Emission factors generally are much less variable than fuel consumption but do change by as much as a factor of two for the flaming and smoldering combustion processes. As a simplifying assumption, for each combustion phase, the emission factor will be assumed to equal a constant. The actual calculations of total emissions production are not done; however, the equations listed in this section contain all of the elements for making emissions production determinations for specified time intervals. The fuel consumption is calculated from the fit equations.

An example of the rate of fuel consumption as a function of time is shown in Figure 7. The fuel consumption as calculated using equation (4) is listed by combustion phase in Table IV. These values are compared to the fuel consumption as measured using an inventory technique.²⁷ The carbon flux technique tends to underestimate the fuel consumption for those fires with lower fuel consumption (Table IV). On the other hand, the measurements of fuel consumption on the units with the highest total fuel consumption are thought to be quite accurate because there was a component of heavier fuels and live vegetation which was consumed but not measured through the inventory.

We have tried fitting different statistical frequency distribution functions to the rate of fuel consumption curves and find that for the data tested we do not develop a good fit. In this analysis, we divide the data into two parts: (1) rate of fuel consumption during the predominantly flaming combustion phase and (2) rate of consumption of fuel during the predominantly smoldering combustion phase. Then a set of generalized equations are defined with limits of integration specific to the combustion phases. Through this process, insight is gained which we believe may link the fuel consumption and emissions source strength phenomena between the flaming and smoldering combustion processes through an exponential growth and decay time constant.

The total emissions production for the fire, e , on a unit area basis (1 square meter) is as outlined by equation (6) and the procedure for assessing total emissions production by time period is given in equation (7):

$$e = e_F + e_s \quad \text{and} \quad (6)$$

$$e = \int_{t_0}^{t_{\max}} f_r(t) (EF_r) dt + \int_{t_{\max}}^{t_{\text{ext}}} f_s(t) (EF_s) dt ; \quad (7)$$

where,

e = total emissions, $g \text{ m}^{-2}$,

e_F = total emissions for the flaming phase, $g \text{ m}^{-2}$,

e_s = total emissions for the smoldering phase, $g \text{ m}^{-2}$,

$f_r(t)$ = a function describing the rate of fuel consumption as a function of time during the flaming phase, $g \text{ m}^{-2} \text{ s}^{-1}$,

EF_r = emission factor for the flaming combustion phase, dimensionless or $g \text{ kg}^{-1}$,

$f_s(t)$ = a function describing the rate of fuel consumption as a function of time during the smoldering phase, $g \text{ m}^{-2} \text{ s}^{-1}$,

EF_s = emission factor for the smoldering combustion phase, dimensionless or $g \text{ kg}^{-1}$,

t_0 = time of ignition, hr,

t_{\max} = time at end of period of maximum rate of combustion, generally also coincident with peak rate of combustion, hr, and

t_{ext} = time at end of smoldering, hr.

The fuel consumption by time period is listed in Table V that corresponds to the integrating periods defined in equation (7). By examining $f_r(t)$ and $f_s(t)$ components of Figure 7 for the MARIA I test, it is observed that as the test progressed that the fuel consumption rate increased markedly and then decreased at an apparent exponential decay rate. Sandberg⁵ has modeled for the total prescribed fire the rate of decay of emissions production as an exponential decay process using the following function:

$$E_s = \int_{t_{\max}}^{t_{\text{ext}}} Q_{\max} \exp(-t/T_{2 \text{ hr}}) dt; \quad (8)$$

where,

t_{ext} , t_{\max} , and E_s are as defined previously and
 Q_{\max} = maximum rate of emissions production, kg s⁻¹,
 $T_{2 \text{ hr}}$ = time decay constant equal to 2 hours, and
 t = integrating variable, time in hours.

The fixed time decay constant shows a reduction in the rate of emissions production of 50% at t equal to 84 minutes. Equation (8) does not have the benefit of the current data base in its formulation. Hence, the relative time constant for the decay parameter is much longer than our data indicates it should be to describe the rate of decrease in smoke production over time. By changing Q_{\max} to q , equation (8) can be modified to a unit area basis as was shown earlier for equation (5). Previously, q was defined as being equal to $\dot{w}EF_{\text{my}}$. For our data, EF_{PM} can reasonably be held constant by selecting the appropriate emission factor for flaming or smoldering combustion. (See Figure 7 and Table III.) Equation (9) describes emissions production, e_s , for a unit area by,

$$e_s = EF_{\text{SPM}} \dot{w}_{\max} \int_{t_{\max}}^{t_{\text{ext}}} \exp(-t/T) dt \quad (9)$$

where, e_s , EF_{SPM} , \dot{w}_{\max} , t_{ext} , t_{\max} , and T have been defined previously and t is the integrating time variable for the smoldering combustion process with limits of integration from t_{\max} to infinity. The integral portion of equation (9) was fitted to the observed fuel consumption curves for the smoldering combustion phase by allowing T to vary incrementally until the results from equation (11) agreed with the measured fuel consumption. All of the parameters used in the fitting process are listed in Table V.

We define e_f similarly except e_f is used to describe a rapidly increasing exponential growth process--the increase in fuel consumption immediately after ignition. The rate of increase in fuel consumption in most cases is much greater during the flaming phase than is the rate of decrease during the smoldering phase. Heat generated during the flaming phase drives moisture from the unburned fuels and in this way extends the consumption during the smoldering combustion phase. The presence of abundant fine fuels may greatly influence the rate of combustion during the startup phase, whereas the larger diameter woody fuels may be important in determining the duration

of the higher rates of combustion. Fuel moisture content is a very important variable in predicting both diameter reduction of woody fuels and consumption of the accumulation of organic material which forms a compact layer of partially decomposed plant parts on the forest floor. The mechanisms for transferring energy between flaming and smoldering combustion phases may be a complex function of all of the above mechanisms. We do not have a sufficient data base from which to deduce these processes. Nevertheless, it is of interest to provide a variable which may prove valuable in linking the smoldering combustion process to the flaming. The following integral was fitted to the flaming phase fuel consumption rate data using a constant value for T for a given fire and allowing K_F (the linkage term) to vary until a "best-fit" was accomplished:

$$e_F = EF_{Fm} \dot{w}_{max} \int_{t_0}^{t_{max}} (1 - \exp(-K_F * t/T)) dt. \quad (10)$$

The solutions to the integrals of equations (9) and (10) are listed in the following two equations and these form the working equations for calculating fuel consumption and emissions production for different intervals of time:

$$e_s = 3.6 EF_{Sm} \dot{w}_{max} T(1 - \exp(-t_s/T)) \quad (11)$$

and similarly,

$$e_F = 3.6 EF_{Fm} \dot{w}_{max} (t + (T/K_F)(\exp(-K_F * t/T) - 1)); \quad (12)$$

where,

e_s , e_F , EF_{Sm} , EF_{Fm} , \dot{w}_{max} have been defined previously and

T = time decay variable which is constant for a given fire,
hr,

K_F = multiplier which sets the rate of increase in fuel
consumption relative to the rate of decrease,

t_s = time from t_{max} to t_{ext} , hr,

t = time from t_0 to t_{max} , hr, and

3.6 = dimensional constant.

The values for T, K_F, \dot{w}_{max} , t_{max} and t_{ext} are listed in Table V and the first derivative for equations (11) and (12) is plotted for each of the four tests in Figure 8 to show the goodness of fit. We do not have data (Table IV) for the flaming phase fuel consumption rate for CAT, hence, K_F has been estimated for that test. For the smoldering fuel consumption function, equation (11), the equation can be evaluated for the conditions tested by multiplying by T since as t becomes large, the exponential component of the equation becomes very small and the bracketed term can be ignored. The total fuel was much lower on CAT since the unit was yarded to a minimum piece size specification of 0.10- x 1.22-m. We used a uniform extinction time of 2.5 hours after

ignition. The time to the end of the maximum fuel consumption period, t_{max} , varied and as discussed previously is believed to be a function of the size and condition of the fuel elements and the ignition procedures.

T and t_{max} may be functions of common variables--if so, T would likely be predictable. The ratio of K_f/T shows that the rate of fuel consumption decay constant for the flaming phase is from 6 to 9 times larger than the decay constant during the smoldering phase. If this ratio holds or if the variability is predictable, then it may be a fairly straight-forward procedure to develop models for predicting fuel consumption as a function of time. Some of the concepts and hypotheses presented here will be tested on independent data sets this summer with the goal of developing further the modeling framework from which emissions from broadcast burning of logging slash can be predicted over the cycle of the fires. These models will help in interpreting the gains in air quality that can be made by altering the fire prescriptions.

CONCLUSIONS

1. A sampling system has been improved for measuring fuel consumption and emissions production--both emission factors and source strength--in real time from undisturbed fuel complexes for broadcast burns of logging slash in western Washington and Oregon. Plans are to complete the characterization of emissions from the broadcast burning of logging slash this year and to develop emissions data for a few other common fuel types of the western United States for which data do not now exist and cannot be readily extrapolated from current research findings.
2. Emission factors for particulate matter without size segregation are substantially in agreement with previously measured emission factors from broadcast burning of logging slash. With the promulgation of a PM-10 air quality standard, the importance of emissions from prescribed burning become more pronounced, as does the need to examine particulate matter emissions as a function of particle size.
3. New emission factors for the flaming phase particulate matter emissions are reported for particles below a mean mass diameter of 2.5 μm . The emission factors average 11.2 ± 3.9 g kg⁻¹ as compared to 16.8 ± 6.3 g kg⁻¹ for open-faced filter mats exposed in the same sample space. Emission factors for the open-faced filter mats are higher than those determined using the 2.5 μm cutpoint cyclone presampler by from 20 to 100+% for the flaming phase and the difference has been found to be a function of reaction intensity.

4. The green fuel component of the fuels has been found to adversely affect emission factors for particulate matter and for benzo[a]pyrene--a polycyclic aromatic hydrocarbon of known carcinogenic properties--so that as the percentage composition of the green fuel that is consumed increases, the size of the emission factors increases for both b[a]p and particulate matter. This is of concern to forest managers because of the need to burn harvested units before planting to reduce the competition of the green vegetation of the seedlings that are being planted.

5. The carbon content of the particulate matter is lower than previously estimated, and particulate matter sampled for broadcast burns of logging slash contains about 50% carbon.

6. The potassium-to-iron ratio ranges over three orders of magnitude and is dependent on combustion efficiency (R-squared of 0.71). There is a need to find a combination of elements or compounds or both that can be used for a reliable indicator of the impact of forest fire smoke at receptor sites.

7. A set of exponential growth-decay equations are fit to the real-world measurements of fuel consumption over time. This should lead to improved models for predicting the response of emissions production for various management actions. Progress is being made in simulating the combined effects of yarding of unmerchantable material to various minimum piece size specifications and the effect of moisture content on the consumption of the fuel and production of emissions. A subsequent paper will be prepared upon the completion of the 1984 work that will elaborate on the findings.

8. Emission factors for trace elements are presented with a linear correlation identified for K as a function of reaction intensity during the flaming phase. EF values for phosphorous remain constant over the same reaction intensity range, EF values for sulfur show a curvilinear relationship. Obviously, many of the thermodynamic parameters affecting the reaction kinetics have not been identified, let alone quantified.

NOTE: This report has not been formally reviewed by the U.S. Environmental Protection Agency, U.S. Department of Energy, or the Bonneville Power Administration; hence, the results and the contents may not necessarily reflect the views and policies of these Agencies.

ACKNOWLEDGMENTS

There are several individuals and agencies to whom we are grateful for their support of this work. The U.S. Environmental Protection Agency, Region X, and the U.S. Department of Energy working through the Pacific Northwest and Alaska Biomass Utilization Task Force are acknowledged for their financial and technical support of this work. The National Forest System personnel at the locations of the prescribed fires were helpful with all phases of the work and especially setting up towers and rigging the cable systems. Jerry White and Charles McMahon, SEFES, Southern Forest Fire Laboratory supplied analytical support, equipment, and methods for sampling particulate matter for b[a]p analysis. Janice Peterson, Kevin Mickelson, James Lopes, and Daniel Bentler are commended for their services in programming the data logger and mainframe computer, and for the technician support provided. Roger Ottmar and Sue Little are acknowledged for providing fuel inventory data and for coordinating the removal of the residues, scheduling and weather forecasting--it wouldn't have been possible without their help.

REFERENCES

1. C. K. McMahon, "Characteristics of Forest Fuels, Fires and Emissions." Presented at 76th Annual Meeting of the Air Pollution Control Association, Atlanta, GA, (June 19-24, 1983).
2. A. A. Marcus, "Prescribed Burning in the Pacific Northwest: Costs and Benefits in Light of the Clean Air Act Visibility Standards." Presented at 76th Annual Meeting of the Air Pollution Control Association, Atlanta, GA, (June 19-24, 1983).
3. Washington Department of Ecology, "Revision to the Washington State Implementation Plan, Washington State's Visibility Protection Program," Washington Department of Ecology, Division of Air Programs, (Feb. 1983).
4. J. A. Cooper, L. A. Currie, and G. A. Klouda, "Assessment of Contemporary Carbon Combustion Source Contributions to Urban Air Particulate Levels Using Carbon-14 Measurements," *Environmental Science and Technology* 15(9):1045-1050 (Sept. 1981).
5. D. V. Sandberg, "Emissions Reduction from Prescribed Forest Burning." Presented at 76th Annual Meeting of the Air Pollution Control Association, Atlanta, GA, (June 19-24, 1983).
6. D. E. Ward, "Source-Strength Modeling of Particulate Matter Emissions from Forest Fires." Presented at 76th Annual Meeting of the Air Pollution Control Association, Atlanta, GA, (June 19-24, 1983).
7. L. Fritschen, H. Bovee, K. Buettner, and others, "Slash Fire Atmospheric Pollution." USDA For. Serv. Res. Pap. PNW-97, 42 pp., Pacific Northwest For. and Range Exp. Stn., Portland, Oregon, (1970).

8. D. E. Ward and R. C. Lamb, "Prescribed Burning and Air Quality--Current Research in the South." Proc. Annu. Tall Timbers Fire Ecol. Conf., August 20-21, 1970, pp. 129-140.
9. R. G. Vines, L. Gibson, A. B. Hatch, N. K. King, and others, "On the Nature, Properties, and Behaviour of Bush Fire Smoke." Div. Appl. Chem. Tech. Pap. No. 1, 32 pp., CSIRO, Australia, (1971).
10. D. V. Sandberg, "Slash Fire Intensity and Smoke Emissions." Presented at the Third National Conference on Fire and Forest Meteorology of the American Meteorological Society and the Society of American Foresters, Lake Tahoe, California-Nevada, (April 2-4, 1974).
11. D. E. Ward, C. C. Hardy, R. D. Ottmar, and D. V. Sandberg. "A Sampling System for Measuring Emissions from West Coast Prescribed Fires." Presented at Pacific Northwest International Section Air Pollution Control Association, Vancouver, BC, Canada, 10 pp. (November 1982).
12. D. V. Sandberg, S. G. Pickford, and E. F. Darley, "Emissions from Slash Burning and the Influence of Flame Retardant Chemicals," *J. Air Pollut. Control Assoc.* 25(3):278-281 (1975).
13. D. E. Ward, H. B. Clements, R. M. Nelson, "Particulate Matter Emission Factor Modeling for Fires in Southeastern Fuels." Sixth Conference on Fire and Forest Meteorology, Society of American Foresters, Seattle, WA, (1980).
14. D. E. Ward, R. M. Nelson, and D. F. Adams, "Forest Fire Smoke Plume Documentation," Presented at the 72nd Annual Meeting of the Air Pollution Control Association, Cincinnati, OH, (June 24-29, 1979).
15. D. E. Ward, E. R. Elliott, C. K. McMahon, and D. D. Wade, "Particulate Source-Strength Determination for Low-Intensity Prescribed Fires." Proceedings Special Conference on Control Technology, Agricultural Air Pollution, Southern Section Air Pollution Control Association, Memphis, TN, pp. 39-54. (March 1974).
16. R. W. Boubel, E. F. Darley, E. A. Schuck, "Emissions from Burning Grass Stubble and Straw," *J. Air Pollut. Control Assoc.* 19: 497-500 (1969).
17. R. M. Nelson, Jr., "An Evaluation of the Carbon Balance Technique for Estimating Emission Factors and Fuel Consumption in Forest Fires," USDA-Forest Service, Research Paper SE-231, 9 pp., Southeastern Forest Experiment Station, Asheville, N.C., (1982).
18. D. E. Ward, D. V. Sandberg, R. D. Ottmar, J. A. Anderson, G. C. Hofer, and C. K. Fitzsimmons, "Measurement of Smoke from Two Prescribed Fires in the Pacific Northwest." Presented at the 75th Annual Meeting of the Air Pollution Control Association. New Orleans, LA, (June 20-25, 1982).
19. D. V. Sandberg and R. D. Ottmar, "Estimating 1000-hour Fuel Moistures in the Douglas-fir Subregion. in *Proceedings, 7th Conference on Fire and Forest Meteorology*, April 25-28, 1983, Ft. Collins, CO.

20. R. D. Ottmar, "Predicting Fuel Consumption by Fire Stages to Reduce Smoke from Slash Fires." Presented at the 1983 Annual Meeting, NW For. Fire Council, Olympia, WA, (November 21-22, 1983).
21. G. M. Byram, "Combustion of Forest Fuels." in *Forest Fire Control and Use*, by K. P. Davis. McGraw-Hill Book Co., Inc., NY, (1959).
22. R. Johnson and C. Huntzicker, "An Automated Thermal Optical Method for the Analysis of Carbonaceous Aerosols," in *Atmospheric Aerosol Sources--Air Quality Relationships* Macis and Hopke, eds., American Chemical Society, Washington, DC, (1981).
23. L. F. Radke, J. H. Lyons, D. A. Hegg, and others, "Airborne Monitoring and Smoke Characterization of Prescribed Fires on Forest Lands in Western Washington and Oregon. EPA 600/X-83-047. Las Vegas, NV, U.S. Environmental Protection Agency. July (1983).
24. P. G. Jenkins, "Aerosol Characterization and Source Determination in the Mt. Rainier Area," Presented at Pacific Northwest International Section of the Air Pollution Control Association, Seattle, WA, (November 1983).
25. D. E. Ward, C. K. McMahon, and D. F. Adams, "Laboratory Measurements of Carbonyl Sulfid and Total Sulfur Emissions from Open Burning of Forest Biomass," Presented at 75th Annual Meeting of the Air Pollution Control Association, New Orleans, LA, (June 20-25, 1982).
26. C. K. McMahon and S. N. Tsoukalas, "Polynuclear Aromatic Hydrocarbons in Forest Fire Smoke," in *Carcinogenesis, Polynuclear Aromatic Hydrocarbons* Vol. 3, P. W. Jones and R. I. Freudenthal, eds., Raven Press, New York, (1978).
27. S. Little and R. D. Ottmar, Pacific Northwest Forest and Range Experiment Station, Seattle, Wa, private communication, (1984).

Table I. Fuel loading, fuel consumption, moisture content of fuel, date of burn, and description of test fires.²⁷

Unit name	YUM Specif. (m x m)	Date burned (1983)	Fuel variables				fuel moisture measured NFDR		
			Preburn		Post burn		---	---	
			woody	duff	woody	duff			
						----- (kg m ⁻²) -----		----- (%) -----	
CAT	0.10 x 1.22	8/19	2.48	13.02	0.43	2.0	27	25	
HEBO	0.15 x 1.83	9/23	4.01	10.06	2.08	3.14	34	24	
MARIA1	0.20 x 3.05	8/21	5.94	17.66	3.59	9.41	31	25	
MARIA2	0.20 x 3.05	9/21	6.41	15.17	3.32	3.79	37	26	
DLAKE1	0.15 x 1.83	7/24	5.51	13.54	3.32	2.31	40	24	
DLAKE2	0.20 x 3.05	9/29	5.72	11.72	3.92	6.43	40	20	

TABLE II. EMISSION FACTORS AND COMBUSTION EFFICIENCY FOR SIX TEST FIRES.

TEST LOCA.	COMBUS. PHASE	CARBON CONC. (mg m ⁻³)	COMB. EFF.	EMISSION FACTORS						REACTION B(a)P INTENSITY (µg kg ⁻¹) (kw m ⁻²)	
				CO ₂	CO	NMHC	CH ₄	PARTICULATE MATTER			
								PM-2.5	PM		
CAT	F	746.	.89	1625	112.	1.1	1.8	13.0	15.4	253	28.9
CAT	S1	216.	.80	1468.	198.	3.2	6.8	17.6	13.8	149	5.0
CAT	S2	65.	.81	1483.	197.	2.8	5.7	9.3	11.7	127	--
HEBO	F	683.	.88	1632.	94.	3.6	4.2	15.9	23.4	298	53.3
HEBO	S1	72.	.77	1413.	231	3.0	7.8	12.4	12.2	448	--
MARIA 1	F	755.	.89	1635.	101.	2.3	2.2	12.2	23.5	694	68.0
MARIA 1	S1	634.	.79	1455.	201.	3.9	7.1	14.0	20.4	297	38.5
MARIA 1	S2	138	.74	1364.	260.	3.4	7.6	12.0	20.3	140	1.0
MARIA 2	F	--	--	--	--	--	--	--	--	--	--
MARIA 2	S1	23.	.63	1146.	359.	2.4	10.0	46.5	34.2	250	--
MARIA 2	S2	34.	.66	1204.	358.	1.2	9.5	18.4	25.8	343	--
DLAKE 1	F	1389	.90	1659.	82.	--	2.8	9.5	10.2	204	48.6
DLAKE 1	S1	144.	.85	1555.	130.	--	5.9	11.7	14.1	252	1.7
DLAKE 1	S2	95.	.77	1403.	156.	--	9.7	11.7	13.4	412	--
DLAKE 1	S3	31.	.69	1261.	177.	--	6.2	9.2	8.1	145	--
DLAKE 2	F	1938.	.94	1720.	56.	1.9	2.2	5.5	11.6	125	83.2
DLAKE 2	S1	268.	.80	1458.	196.	4.6	19.4	11.4	14.1	257	10.0
DLAKE 2	S2	75.	.78	1427.	222.	3.6	8.4	12.7	12.4	228	--

TABLE III. EMISSION FACTORS FOR TRACE ELEMENTS FOR SIX TEST FIRES IN WESTERN OREGON (1983).

TEST LOC.	EMISSION FACTORS										RATIO ANALYSIS			
	Al	Si	P	S	Cl	K	Ca	Mn	Fe	K/Fe	K/PM	Fe/PM	S/PM	
(mg kg ⁻¹)										(dimensionless)				
CAT F	13.3	12.2	8.3	26.5	73.9	76.6	26.1	2.3	4.1	18.7	5.9	0.3	2.0	
CAT S1	8.0	9.6	4.0	26.4	32.9	26.0	10.0	0.8	2.4	10.8	1.5	0.1	1.5	
CAT S2	64.8	120.8	8.6	28.3	20.5	26.9	69.0	8.9	49.6	.5	2.9	5.3	3.0	
HEBO F	16.1	17.4	11.8	64.0	167.6	311.7	4.8	1.3	2.8	111.3	19.6	0.2	4.0	
HEBO S1	17.2	28.6	5.1	21.6	19.1	20.3	1.9	0.2	3.0	6.8	1.5	0.2	1.7	
MARIA1F	20.0	23.0	8.5	45.8	127.9	161.4	12.1	0.7	4.7	34.3	13.2	0.4	3.8	
MARIA1S	5.0	5.2	4.9	11.7	27.8	23.9	6.9	0.3	2.0	12.0	1.7	0.1	0.8	
MARIA1S	--	--	--	--	--	--	--	--	--	--	--	--	--	
MARIA2F	--	--	--	--	--	--	--	--	--	--	--	--	--	
MARIA2S	36.9	175.5	23.1	13.9	--	32.3	67.0	9.2	78.5	0.4	0.7	1.7	0.3	
MARIA2S	13.5	21.7	9.5	3.7	34.0	11.0	22.6	1.8	4.6	2.4	0.6	0.3	0.2	
DLAKE1F	5.4	4.5	3.9	26.6	29.7	95.2	7.4	0.7	0.3	317.3	10.0	0.0	2.8	
DLAKE1S	13.8	39.4	1.9	12.9	5.3	17.2	21.0	1.9	9.1	1.9	1.5	0.8	2.2	
DLAKE1S	10.3	33.3	1.2	12.7	4.0	11.5	6.7	1.2	6.3	1.8	1.0	0.5	1.1	
DLAKE1S	--	--	--	--	--	--	--	--	--	--	--	--	--	
DLAKE2F	16.8	11.0	11.4	31.7	38.9	133.8	44.5	4.3	1.9	70.4	24.3	0.4	5.8	
DLAKE2S	9.8	12.0	3.1	4.2	4.2	24.6	7.5	0.2	3.4	7.2	2.2	0.3	0.4	
DLAKE2S	--	--	--	--	--	--	--	--	--	--	--	--	--	
						Mean				42.6	6.2	0.8	2.1	
						Standard deviation				±85.3	±7.7	±0.8	±2.1	
						Coefficient of variation				200%	125%	181%	77%	

NOTE TO EDITORS

Under the new federal copyright law,
publication rights to this paper are
retained by the author(s).

Table IV. Total fuel consumed per square meter by two independent measurement techniques.

TEST Unit	INV ^{a27} W	Total Fuel Consumed CFX ^a			Difference CFX ^a vs. INV -(%)
		W _F	W _S	W	
CAT	9.1	2.7	4.9	4.9+2.7**	-16
HEBO	5.6	1.3	2.3	3.6	-35
MAR	14.0	8.5	16.8	25.3	+81
DL2	11.1	6.2	9.6	13.7+2.1***	+23

* INV = inventoried fuel consumption.

CFX = carbon-flux fuel consumption (W_F = fuel consumption for flaming, W_S = fuel consumption for smoldering, and W = total fuel consumption).

**Sampling did not begin immediately (see figure 8). It is estimated that the unmeasured fuel consumption was 2.1 kg m⁻².

***Estimate of tail region not calculated from carbon flux data. Measurement calculations stopped at 1.5 hours.

Table V. Parameters and values used in fitting equations to the observed rates of fuel consumption for four units.

Unit	\dot{W}_{max} (g/m ² /s)	t_{max}	t_{ext}	T	K _F	K _F /T	W _F	W _S
			(hour)		(dimens)	(1/hour)		(kg/m ²)
CAT	3.9	.33	2.5	.350	2.3	6.6	2.70	4.89
HEBO	7.6	.12	2.5	.086	0.8	9.3	1.25	2.33
MARIA1	7.7	.45	2.5	.632	4.2	6.7	8.50	16.83
DLAKE2	7.7	.33	2.5	.346	3.2	9.3	6.24	9.56

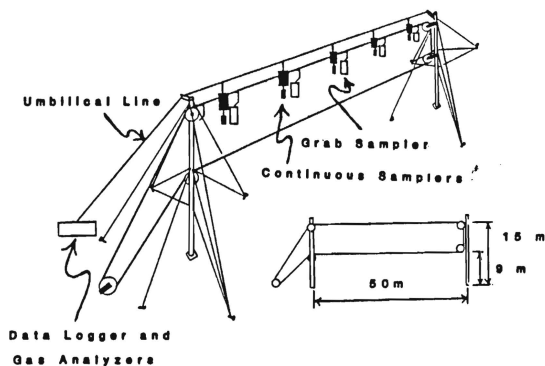


Figure 1. Cables and towers used to support two sets of packages over prescribed fires for continuous sampling of emissions and for collecting grab samples of emissions from the same sample space.

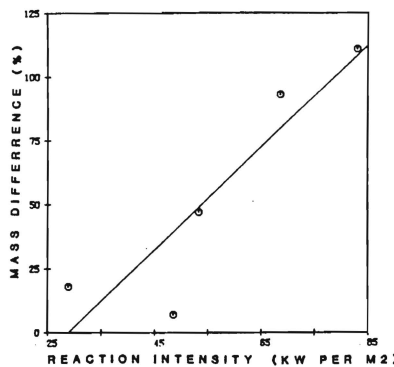


Figure 2. Percent difference between emission factors determined from gravimetric samples of PM collected on open-faced 47-mm filters and 37-mm filters (with 2.5 μ m cutpoint presample) as a function of IR.

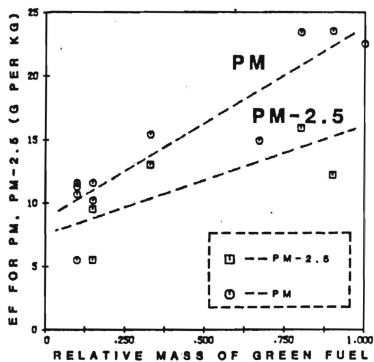


Figure 3. A general increase in particulate matter emission factors is observed as relative green fuel abundance increases.

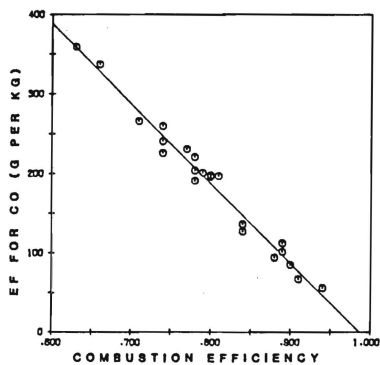
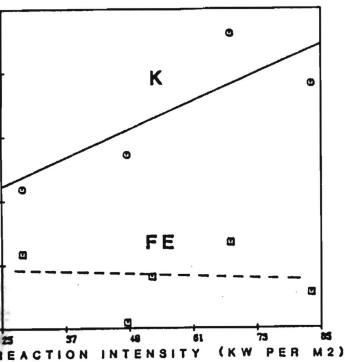


Figure 4. CO emission factors are a function of combustion efficiency.



5a. The relative magnitude of K and Fe emission factors as a function of reaction intensity. EF_K is correlated with IR with squared $r = 0.69$.

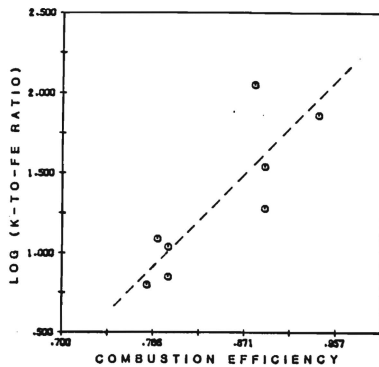
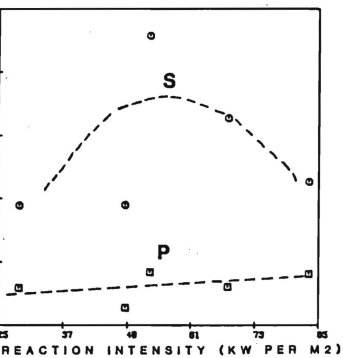


Figure 5b. K/Fe ratio values range over three orders of magnitude and are correlated with combustion efficiency.



5c. Sulfur emission factors are hypothesized to vary curvilinearly, whereas phosphorous shows a linear trend.

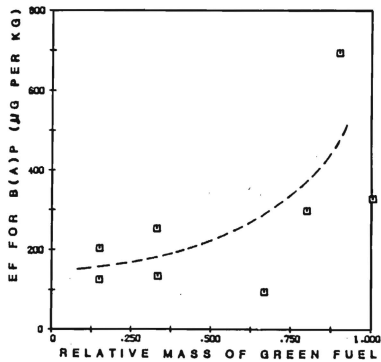


Figure 6. Emission factors for b[a]p during the flaming phase are generally higher for those test units with the largest live fuel component.

Figure 7. Continuum of measured values of fuel consumption, temperature, vertical velocity of the smoke plume, and combustion efficiency; emission factors for CO, CO₂, and PM; and source strength for CO and PM (data for MARIA 1).

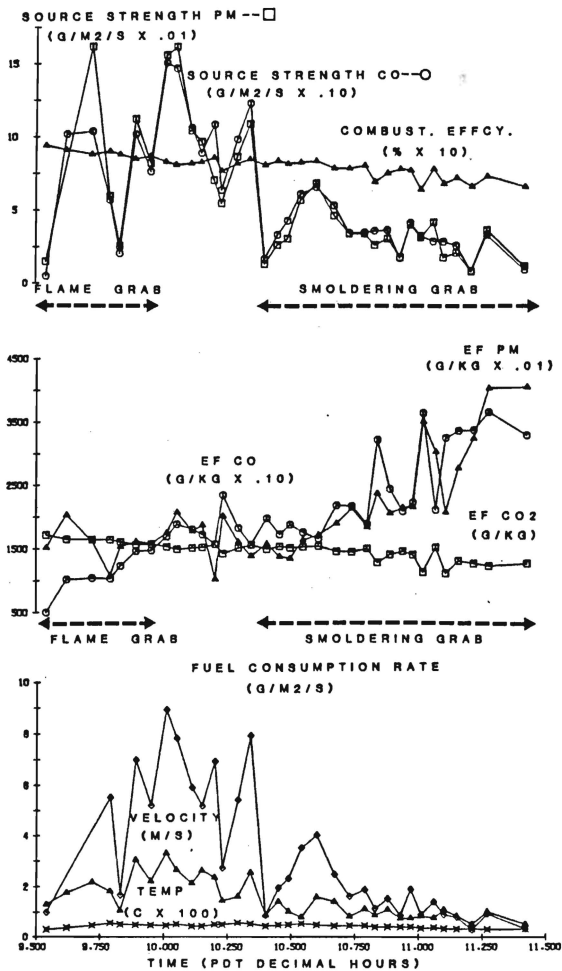


Figure 8. The fitted representation of the measured fuel consumption rate as a function of time for the flaming and smoldering combustion phases for four units. Both fuel moisture content and the mass of woody fuel affect the rate and duration of fuel consumption.

